Supplementary Figure Legends

Figure S1. Alignment of chicken erythrocyte βVI tubulin (CβVI) sequence with major bovine brain βII tubulin (BβII) and major human βI tubulin (HβI) sequences. All sequence divergences are highlighted in grey. Sequence differences that result in most significant changes in amino acid side chain are marked with an asterisk. Divergences involved in primary contacts with Taxol and/or discodermolide are boxed. Secondary structure designations are shown below the alignment, with Sn representing β-sheets and Hn representing α-helices.

Figure S2. GTP-free assembly of (a) chicken erythrocyte tubulin (CET) and (b) bovine brain tubulin (BBT) in the presence of Taxol and discodermolide. CET and BBT, stored in a GTP-free buffer containing 3M glycerol, were brought to 1.0 mg/mL (10 μM). After equilibration at 37^{o}C, 10 μM drug or an equal volume of DMSO (control) was added, and the absorbance at 350 nm was monitored for 40 min. Arrows indicate points at which the corresponding drug was added. Assembly in the presence of DMSO is shown as a thin solid line, in the presence of discodermolide as a thick solid line, and in the presence of Taxol as a dashed line.

Figure S3. Representative mass spectra of isobaric α- and β-tubulin peptides. Sequence coverage was determined based on FT-MS data with mass accuracy threshold of ≤2 ppm. Isobaric peptides, those whose masses are identical, but sequences different, were identified by MS/MS analysis. Shown here are representative LTQ-MS (I), MS/MS (II), FT-MS at 0 min HDX (III), and FT-MS at 30 min HDX in the presence of discodermolide (IV) for one α-tubulin peptide, α287-294 (a), and one β-tubulin peptide, β341-353 (b).

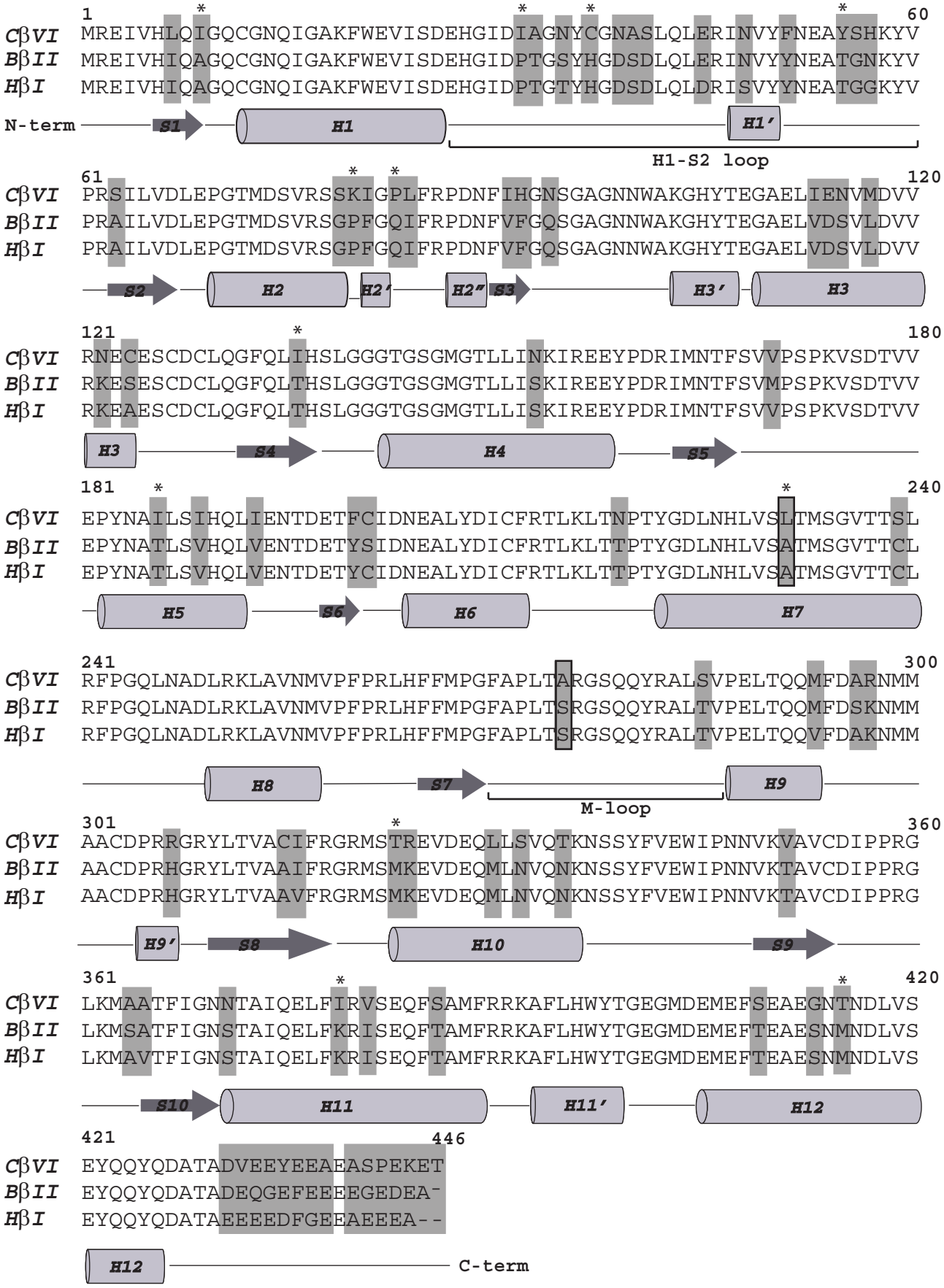
1
60
CβVI MREIVHLQIGQCGNQIGAKFWEVISDEHGIDIAGNYCGNASLQLERINVYFNEAYSHKYV
BβII MREIVHIQAGQCGNQIGAKFWEVISDEHGIDPTGSYHGDSDLQLERINVYYNEATGNKYV
HβI MREIVHIQAGQCGNQIGAKFWEVISDEHGIDPTGTYHGDSDLQLDRISVYYNEATGGKYV
N-term
S1
H1
H1′
H1-S2 loop
61
120
CβVI PRSILVDLEPGTMDSVRSSKIGPLFRPDNFIHGNSGAGNNWAKGHYTEGAELIENVMDVV
BβII PRAILVDLEPGTMDSVRSGPFGQIFRPDNFVFGQSGAGNNWAKGHYTEGAELVDSVLDVV
HβI PRAILVDLEPGTMDSVRSGPFGQIFRPDNFVFGQSGAGNNWAKGHYTEGAELVDSVLDVV
S2
H2
H2′
H2″
S3
H3′
H3
121
180
CβVI RNECESCDCLQGFQLIHSLGGGTGSGMGTLLINKIREEYPDRIMNTFSVVPSPKVSDTVV
BβII RKESESCDCLQGFQLTHSLGGGTGSGMGTLLISKIREEYPDRIMNTFSVMPSPKVSDTVV
HβI RKEAESCDCLQGFQLTHSLGGGTGSGMGTLLISKIREEYPDRIMNTFSVVPSPKVSDTVV
H3
S4
H4
S5
181
240
CβVI EPYNAILSIHQLIENTDETFCIDNEALYDICFRTLKLTNPTYGDLNHLVSLTMSGVTTSL
BβII EPYNATLSVHQLVENTDETYSIDNEALYDICFRTLKLTTPTYGDLNHLVSATMSGVTTCL
HβI EPYNATLSVHQLVENTDETYCIDNEALYDICFRTLKLTTPTYGDLNHLVSATMSGVTTCL
H5
S6
H6
H7
241
300
CβVI RFPGQLNADLRKLAVNMVPFPRLHFFMPGFAPLTARGSQQYRALSVPELTQQMFDARNMM
BβII RFPGQLNADLRKLAVNMVPFPRLHFFMPGFAPLTSRGSQQYRALTVPELTQQMFDSKNMM
HβI RFPGQLNADLRKLAVNMVPFPRLHFFMPGFAPLTSRGSQQYRALTVPELTQQVFDAKNMM
H8
S7
H9
M-loop
301
360
CβVI AACDPRRGRYLTVACIFRGRMSTREVDEQLLSVQTKNSSYFVEWIPNNVKVAVCDIPPRG
BβII AACDPRHGRYLTVAAIFRGRMSMKEVDEQMLNVQNKNSSYFVEWIPNNVKTAVCDIPPRG
HβI AACDPRHGRYLTVAAVFRGRMSMKEVDEQMLNVQNKNSSYFVEWIPNNVKTAVCDIPPRG
H9′
S8
H10
S9
361
420
CβVI LKMAATFIGNNTAIQELFIRVSEQFSAMFRRKAFLHWYTGEGMDEMEFSEAEGNTNDLVS
BβII LKMSATFIGNSTAIQELFKRISEQFTAMFRRKAFLHWYTGEGMDEMEFTEAESNMNDLVS
HβI LKMAVTFIGNSTAIQELFKRISEQFTAMFRRKAFLHWYTGEGMDEMEFTEAESNMNDLVS
S10
H11
H11′
H12
421
446
CβVI EYQQYQDATADVEEYEEAEASPEKET
BβII EYQQYQDATADEQGEFEEEEGEDEA-
HβI EYQQYQDATAEEEEDFGEEAEEEA--
H12
C-term

Figure S1

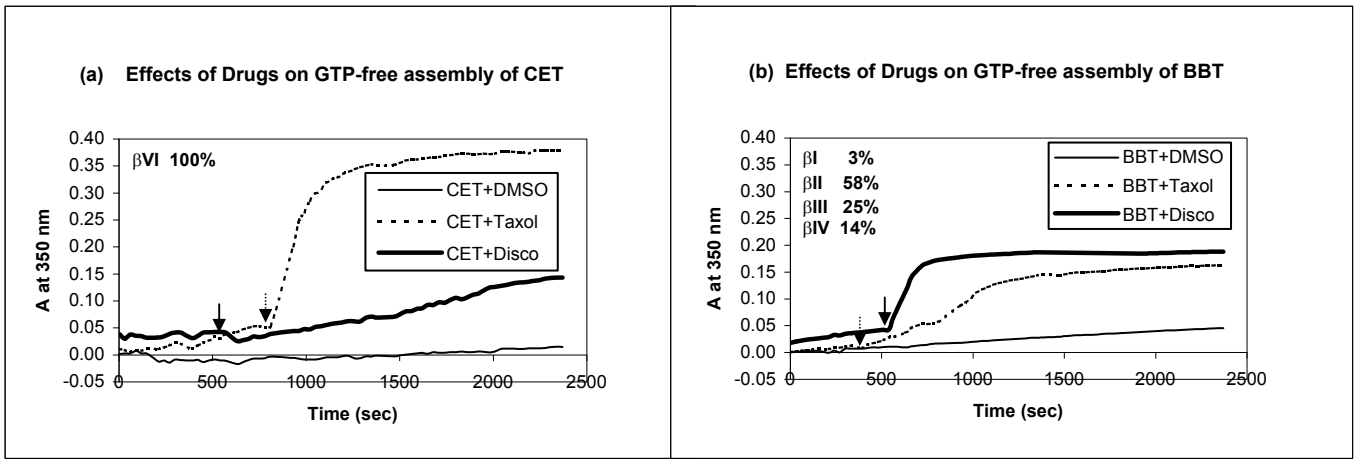
(a) Effects of Drugs on GTP-free assembly of CET
βVI 100%
CET+DMSO
CET+Taxol
CET+Disco
A at 350 nm
Time (sec)
(b) Effects of Drugs on GTP-free assembly of BBT
βI 3%
βII 58%
βIII 25%
βIV 14%
BBT+DMSO
BBT+Taxol
BBT+Disco
A at 350 nm
Time (sec)

Figure S2

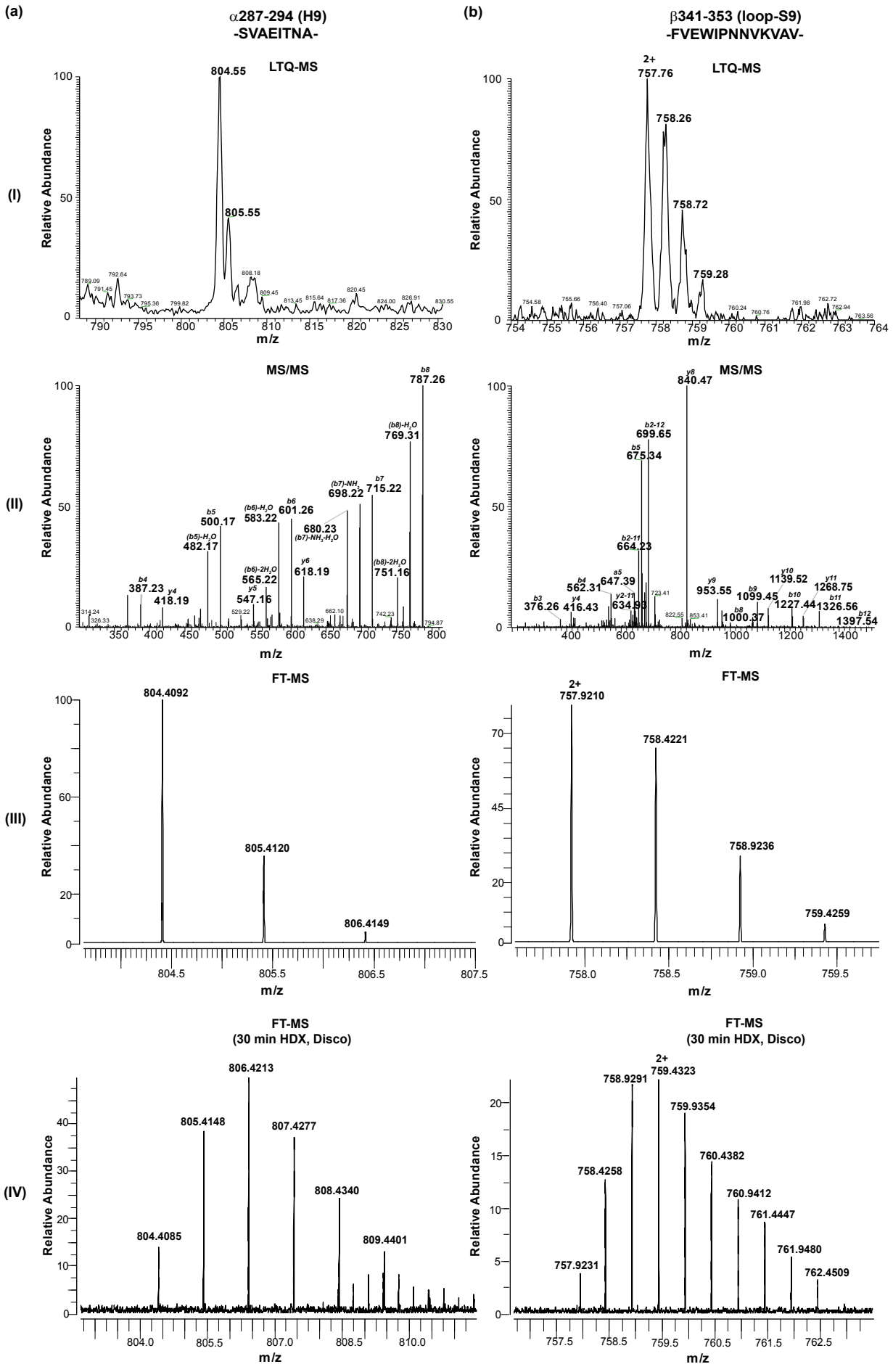
(a)
α287-294 (H9)
-SVAEITNA-
(b)
β341-353 (loop-S9)
-FVEWIPNNVKVAV-
(I)
LTQ-MS
804.55
805.55
2+
757.76
758.26
758.72
759.28
(II)
MS/MS
787.26
769.31
715.22
698.22
601.26
583.22
500.17
482.17
680.23
618.19
565.22
547.16
418.19
387.23
751.16
840.47
699.65
675.34
664.23
647.39
562.31
953.55
1139.52
1268.75
1227.44
1326.56
1099.45
1000.37
1397.54
(III)
FT-MS
804.4092
805.4120
806.4149
2+
757.9210
758.4221
758.9236
759.4259
(IV)
FT-MS
(30 min HDX, Disco)
806.4213
805.4148
807.4277
808.4340
804.4085
809.4401
2+
759.4323
758.9291
759.9354
760.4382
758.4258
760.9412
761.4447
761.9480
757.9231
762.4509
Relative Abundance
m/z

Figure S3